Lithospheric Structure of the Eastern Paraná Basin of Central Brazil From Surface-Wave Inversion Comparing Genetic Algorithms and Linearized Least-Squares Inversion

Kai Zhang and Arthur Snoke
Department of Geological Sciences, Virginia Tech

David James
Department of Terrestrialal Magnetism
Carnegie Institution of Washington

GREAT-CIRCLE PATHS ACROSS EASTERN PARANA BASIN

Figure 1: A schematic outline of the major geological provinces in southern Brazil, the locations of broadband BLSP stations, and great-circle trajectories for surface-wave paths with interstation segments traversing the eastern Paraná Basin. Recording systems consisted of 3-component broadband Streckeisen STS-2 seismometers and dual-gain, 16-bit REFTEK data loggers with GPS timing and location.

Figure 2: Vertical, radial and transverse components for event 92333 recorded at station PPDB (left: Δ = 2262 km) and event 94043 recorded at TRIB (right: Δ = 8310 km). Paths and stations are labeled in Fig. 1. Time traces have been decimated and instrument corrected. Note the near-perfect separation of Rayleigh and Love waves on the horizontal components and, for event 92333, the absence of signal soon after the arrival of the large-amplitude (minimum group velocity) Airy phase.

Figure 3: Frequency-time (group-velocity) analysis for the instrument-corrected, vertical-component seismograms from the two events shown in Fig. 2. The x's are computer-picked maxima for selected periods, and the vertical lines are ±1 dB. Contours are spaced every 3 dB. The period range is 10–137 s for event 92333 and 30–198 s for event 94043.

The JGR97 Study

As reported earlier (JGR v 102, pp 2939–2951, 1997), surface-wave data from a portable broadband array have been used to invert for the one-dimensional velocity structure of the crust and upper mantle beneath the eastern Paraná Basin in central Brazil (see Figure 1). The inversion was based on interstation phase and group velocities for fundamental and first higher mode Rayleigh waves and fundamental mode Love waves from seven events. (Figure 2 shows sample waveforms, figure 3 frequency-time analyses from the vertical-component seismograms for those events, and figure 4 shows the set of dispersions derived from the data set and the final velocity structure -- PARANA-F.) The average Moho depth was found to be about 42 km, and the cratonic upper-mantle to be characterized by high velocities with a maximum S-wave velocity of 4.7 km/s and no resolvable low-velocity zone to at least 200 km depth. Results from receiver function analysis were used to help constrain the crustal structure and Moho depth.
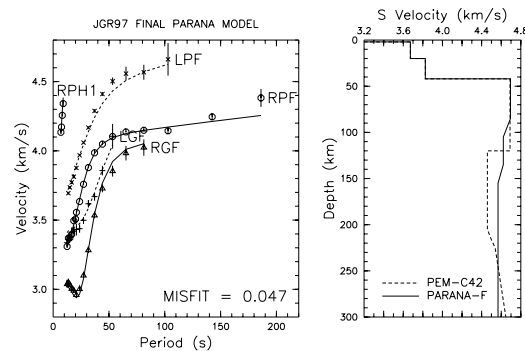

Figure 4: Eastern Paraná interstation phase and group velocities vs period are shown on the left for the seven events used in the inversion for S-wave velocity. Fundamental Rayleigh-wave velocities were used for all seven events, first-higher-mode Rayleigh phase velocity for one event, and fundamental Love-wave velocities for four events. Individual event dispersion values were interpolated at a set of selected periods and then both the velocities and their standard errors were averaged. Line curves are calculated from the velocity model after inversion and are labeled according to **R**ayleigh/**L**ove, **P**hase/**G**roup, **F**undamental/**H**igher-mode. The final velocity-depth model (PARANA-F) is shown on the right. Model PEM-C42 is included for reference: it is model PEM-C [Dziewonski et al., 1975] mantle with the PARANA crust. The displayed model layer transitions have been smoothed except for intended first-order discontinuities.

Concluding Remarks

GA will not replace LLSI, but it can supplement it as a means to map out the model space for resolution and uniqueness. Further, GA can combine different data sets, such as surface waves and receiver functions.

Linearized Least-Squares Inversion

The S-wave structure was derived using Herrmann's linearized least-squares inversion (LLSI) program SURF. Forward modeling stability requires thin (10-20 km thick) constant-velocity layers, and, in SURF, each S-wave layer value is a model parameter. A flatness constraint is employed to limit the size of changes in adjacent-layer model values. As a consequence, the matrix to be inverted is ill-conditioned -- only three eigenvalues of the 43 are greater than 0.1 times the maximum --, and the requisite damping couples model parameters reducing the model resolution and providing underestimates of the model variances -- e.g., the variance estimates in PARANA-F at 300 km depth are less than in the crust, and the depth resolution is more than 100 km.. Hence it is difficult to quantify the existence of a low-velocity zone at depths greater than 100 km. Further, the nonlinearities between data and model parameters provide little guarantee of model uniqueness.

Genetic Algorithms: Background

The only true way to quantify the constraints on the velocity structure imposed by a data set as shown in Fig. 4 is to employ a full Monte Carlo forward modeling analysis of the model space. To achieve a useful resolution in depth and velocity would be impracitically time consuming. Genetic Algorithms (GA) is one of a new class of fully nonlinear global optimization techniques. Presented here are applications of a GA approach based on Sandbridge & Callagher (1991), to which we refer for details.

In a GA, one constructs a model parameterization represented by a string of bits resulting from a discretization of the model space. The initial population of models is Q bit-strings generated randomly (from perturbations of a starting model). One also establishes a misfit criterion. GA is an iterative process in which each step has three stages: selection, crossover and mutation. **Selection** chooses from among the current model population: we use S&G's tournament selection procedure. **Crossover** exchanges parts of bit-strings between pairs of models: we cross over individual model parameters rather than simply a range of bits. **Mutation** randomly changes individual bits: we do not weight the probability according to bit order.

As we were not interested primarily in the single best model, but rather all the models generated which satisfied a misfit criterion, we kept all models generated from all iterations and sorted them by misfit. We found the initial population to matter, so we repeated runs with different random seeds. We also tried runs with different probabilities (see S&G).
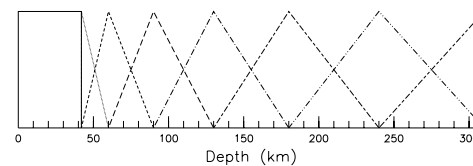

Figure 5: Interpolation model parameters (termed basis functions by Nolet [1990]) used in GA. The single parameter covering the crust is "box car" in shape, resulting in uniform weighting throughout the depth range. The upper mantle, from 42 km to 310 km, is spanned by seven overlapping triangles with widths increasing with depth, reflecting the decreasing model resolution with increasing depth. Velocities for depths greater than 310 km, below the depth range resolved by these data, have the same perturbation as the velocity at 310 km.

Genetic Algorithms: Results

Our misfit criterion uses the RMS observed-calculated data misfit supplemented by a model smoothness constraint. Although we use the thin-layer velocity structure for forward modeling, we combine these into fewer parameters for GA (Fig. 5). Our final parameter set (8) is less than our initial set because separate crustal parameters tracked closely. We chose not to have the Moho depth as a separate parameter because of tradeoffs: we did separate runs with different Moho depths. Our number of bit-strings (Q) was 32, and the bit-string length was 63, with crustal velocities varying by ± 0.6 km/s and crustal velocities by ± 0.3 km/s from our starting model (PARANA-F for runs shown).

The results shown are preliminary, but they demonstrate the power of GA to show which parts of the model space are better constrained than others (Fig. 6), and the tools developed can be applied to test quickly the relative sensitivities of parts of the model space to a given data set (Fig. 7). For the data set in this study, the crustal velocities are well constrained as is the fact that the uppermost mantle has high velocities (Fig. 6). Velocities at depths greater than 150 km are not well constrained (Figs. 6, 7)
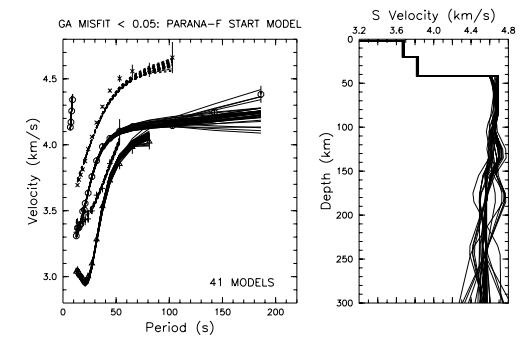

Figure 6: Dispersions and velocity models generated by GA with misfits less than 0.05 and no mantle velocity discontinuities of more than 0.1 km/s over 10 km. The starting model is PARANA-F, the final model from the JGR97 study based on least-squares inversion. Shown are the composite of results from three GA runs. Note that the crustal velocities have a small variation among models, but in the mantle the range in velocities increases with depth.
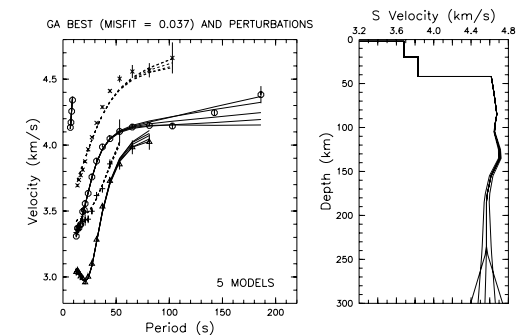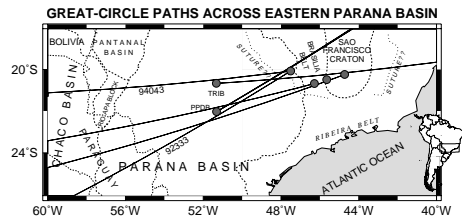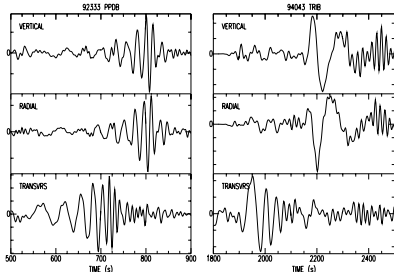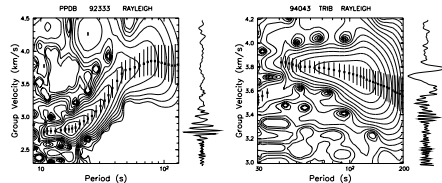

Figure 7: Dispersions and velocity model for lowest misfit from GA runs (Fig. 6) and dispersions produced by perturbing that model at greater depths. Calculated Rayleigh phase velocities at the higher periods increase as the S -wave velocity at greater depths increases. Given the increased estimated errors in dispersion for the higher periods, none of these models can be ruled out, and all lead to smaller misfits than does PARANA-F.